Elastic stiffness of the nuclear-spin system in tetragonal U2D2 nuclear-ordered solid He-3

AUTHOR(S):

Yamaguchi, M; Sasaki, S; Lee, SG; Sasaki, Y; Mizusaki, T

Elastic Stiffness of the Nuclear-Spin System in Tetragonal U2D2 Nuclear-Ordered Solid ^{3}He

M. Yamaguchi, S. Sasaki, S. G. Lee, Y. Sasaki, and T. Mizusaki
Department of Physics, Graduate School of Science, Kyoto University, Kyoto 606-8502, Japan
(Received 7 March 2003; published 9 September 2003)

We have measured temperature dependences of sound velocity for both longitudinal and transverse sound in nuclear-ordered U2D2 solid ^{3}He with several crystal orientations along the melting curve. The sound velocity change was proportional to T^4 for all sound modes and crystal orientations and was attributed to the nuclear-spin part of the internal energy. We extracted six-independent elastic stiffness of the nuclear-spin part and obtained Grüneisen constants of the spin wave velocity for four-independent strains. Grüneisen constants for compressional strain were larger than those for shear strain. Using the multiple-spin-exchange model, we explain the anisotropy of Grüneisen constants in tetragonal symmetry.

DOI: 10.1103/PhysRevLett.91.115301 PACS numbers: 67.80.Cx, 67.80.Jd

The nuclear magnetism of solid ^{3}He is a prototype system to study fundamental properties of exchange processes in magnetism where the atomic exchange process can be calculated from first principles [1]. The multiple-spin-exchange model, particularly the three-parameter model with the nearest neighbor exchange J_{NN}, the three-body J_T, and the four-body planar exchange K_P, has been proposed to describe the nuclear magnetism of solid ^{3}He [2]. However, it was pointed out that the five-body, the six-body, and even the higher-order exchange processes were needed for quantitative discussion. Recently, a new model for the ^{3}He nuclear magnetism was proposed, which was based upon the nuclear-spin-exchange interaction through the 2P-state electron dipolar interaction caused by the correlated zero point motion of ^{3}He atoms [3]. In this Letter, we still use the multiple-spin-exchange model and analyze the anisotropy of sound velocity in U2D2 solid ^{3}He.

One of the important features of the exchange interaction in solid ^{3}He nuclear magnetism is that the exchange constants, denoted typically by J, are very strongly dependent on the molar volume, where Grüneisen constants for various exchange processes J are defined as $\gamma^J = \frac{d\ln J}{d\ln V}$. The molar volume dependences of some thermodynamic quantities such as the nuclear-ordering temperature T_N, the critical fields Bc_1 and Bc_2, and the Curie-Weiss temperature θ_W have been measured and the Grüneisen constants for those quantities are similar to each other, and are about 20 [4]. The small difference in Grüneisen parameters is attributed to differences in the Grüneisen constants for various multiple exchange parameters. It is very desirable and important in ^{3}He nuclear magnetism to obtain the Grüneisen constants for various multiple exchange parameters for various directions of uniaxial stress and shear stress.

It was reported that the ultrasound was strongly coupled to the nuclear-spin system through large Grüneisen constants of exchange parameters and the temperature-dependent sound velocity below a few mK [5] and even at high temperatures [6] was directly related with nuclear-spin internal energy and the Grüneisen constants. Nomura *et al.* [5] analyzed data of longitudinal sound velocities at 11 MHz by using an approximation of a homogeneous medium. Neglecting anisotropy of sound velocity in the nuclear ordered U2D2, they derived a Grüneisen constant $\gamma^{\langle c\rangle}$ for the spin wave velocity $\langle c\rangle$ to be 16. In this report, we measured longitudinal and transverse sound velocities simultaneously for 15 different crystals in the U2D2 phase along the melting pressure with much better accuracy than the previous measurement and obtained six-independent elements of elastic stiffness of the nuclear-spin part in the tetragonal U2D2 phase from the temperature-dependent part of sound velocity. We derived the general expression for nuclear-spin-dependent anisotropy of elastic stiffness in U2D2 solid ^{3}He from the multiple-spin-exchange model and compared it with observed anisotropy of sound velocities in the tetragonal symmetry.

A single crystal of U2D2 solid ^{3}He usually has three magnetic domains, and a single domain crystal is necessary to study the anisotropy of the sound propagation in the U2D2 phase. By using a method similar to Ref. [5], we made 15 crystals with an almost single magnetic domain (more than 70% occupied by one of the domains) from about 30 crystals grown. We grew a crystal in superfluid ^{3}He-B in a narrow space between two parallel transducers with 3 mm separation, one of which was a Z-cut $LiNbO_3$ for a longitudinal wave and the other was a X-cut crystal for a transverse wave. We could measure simultaneously all three sound modes in the crystal but slow transverse mode was often not observed, depending on the crystal orientation and the geometry of the sample cell. The fundamental frequencies of the transducers were 7.5 MHz for the longitudinal sound and 3.6 MHz for the transverse sound, and both sound signals were measured up to about 50 MHz by using the higher harmonics of the transducers. We measured sound velocity and attenuation by the pulse echo method with phase sensitive detection

below the nuclear-ordering temperature $T_N = 0.93$ mK [7]. Two transducers were parallel to each other within an accuracy of 1 μm in the active area of the sound transducer of 10 mm^2, estimated from interference patterns of echoes and we could typically observe about 100 sound echoes for 7.5 MHz longitudinal sounds. Attenuation of the sound increased rapidly as frequency and temperature increased and will be reported elsewhere. The absolute values of the sound velocity v were determined from the time of flight of sound between echoes with 0.5% accuracy. The relative changes of sound velocity $\frac{\Delta v}{v}$ were measured from the phase difference between sound echoes using a phase sensitive detection with 10^{-5} resolution.

The U2D2 spin structure has a uniaxial symmetry which has an anisotropy axis $\hat{l}$ along the [100] or equivalent axes. We determined by cw-NMR the crystal orientation from the part of the sample with three domains and the temperature of solid samples, using the Osheroff-Cross-Fisher equations [Eqs. (2) and (3) and Ref. [8]], where the magnetic field was applied parallel to the sound propagation direction $\hat{k}$. We specify the crystal orientation (θ, ϕ), where θ is the angle between $\hat{l}$ (we choose $\hat{l} \parallel \hat{z} = [001]$) and $\hat{k}$, and ϕ is the azimuthal angle of $\hat{k}$ measured from $\hat{x} = [100]$.

Sound velocities are described by the elastic stiffness c_{ij}. We divided c_{ij} into two parts,

$$c_{ij} = c_{ij}^L + c_{ij}^N(T). \tag{1}$$

The first term c_{ij}^L is the temperature-independent part and comes almost from the lattice energy (only about 0.1% of c_{ij}^L is the contribution from the temperature-independent spin energy and is negligible). The second term $c_{ij}^N(T)$ is the temperature-dependent nuclear-spin part. The elastic stiffness generally has 21 components and the number of independent components reduces to three, c_{11}, c_{12}, and c_{44}, in cubic symmetry (the lattice parts) and reduce to six, c_{11}, c_{33}, c_{12}, c_{13}, c_{44}, and c_{66}, in tetragonal symmetry (the U2D2 spin parts), where i and j in c_{ij} denote 1:xx, 2:yy, 3:zz, 4:yz, 5:xy, 6:zx. We determined the lattice parts to be $c_{11}^L = 2.21$, $c_{12}^L = 1.84$, $c_{44}^L = 1.08$ [10^8 g/cm s^2] for bcc solid ^{3}He at the melting pressure (24.2 [cm^3/mol]) from v and are tabulated in Table I. These values are in good agreement with Wanner's values [9] almost within the three above digits. Typical temperature dependence of the relative changes of sound velocity $\frac{\Delta v}{v}$ for three sound modes, one longitudinal and fast and slow transverse sounds are shown in Fig. 1. The sound velocity change was proportional to T^4 for all sound modes and all crystal orientations. We fitted the data to

$$\frac{\Delta v}{v} = A_P(\theta, \phi)\left(\frac{T}{T_N}\right)^4. \tag{2}$$

The coefficient, A_P, depends on θ and ϕ and the sound mode P. It should be noted that the coefficient A_P did not depend on the sound frequencies between 3 and 50 MHz within our experimental accuracy, and the coupling of sound with collective spin waves was not observed at the few frequencies of this experiment [10]. Since we measured the velocity change along the melting curve, the velocity of the lattice part changes as $[\Delta v(V_{\rm mol})]/v$ due to the change of molar volume along the melting curve. We subtracted it from $\frac{\Delta v}{v}$ in order to obtain the nuclear-spin part of the sound velocity. The velocity change $[\Delta v(V_{\rm mol})]/v$ is expected to be isotropic and, since $\Delta V_{\rm mol}$ is proportional to T^4[11], is given by

$$\frac{\Delta v(V_{\rm mol})}{v} = \left(\gamma_L + \frac{1}{3}\right)\frac{\Delta V_{\rm mol}}{V_{\rm mol}} = B\left(\frac{T}{T_N}\right)^4, \tag{3}$$

where γ_L is the Grüneisen constant of sound velocity and $\Delta V_{\rm mol}$ is the molar volume change along the melting curve. Using $\gamma_L = -2.2$ [9], $\Delta V_{\rm mol} = -4.0 \times 10^{-4}(\frac{T}{T_N})^4$ [11], we obtained $B = 0.31 \times 10^{-4}$. The $[\Delta v(V_{\rm mol})]/v$ was at most 30% of the $\frac{\Delta v}{v}$ below T_N. We subtracted the above contribution from the measured value of $A_P(\theta, \phi)$ and obtained the nuclear-spin part of the sound velocity as follows:

$$C_P(\theta, \phi) = A_P(\theta, \phi) - B. \tag{4}$$

Measured values of $C_P(\theta, \phi)$ for 15 crystals are shown in the stereograph plot in Fig. 2. Typical values of $C_P(\theta, \phi)$ were in the order of 10^{-4}.

From the $C_P(\theta, \phi)$, we extracted the six-independent elements of c_{ij}^N, where $c_{ij}^N(T) = c_{ij}^N(T/T_N)^4$, subtracting the value of c_{ij}^L. We obtained c_{ij}^N to be $c_{11}^N = 3.4 \pm 1.0$, $c_{33}^N = 7.4 \pm 1.0$, $c_{12}^N = 4.7 \pm 1.7$, $c_{13}^N = 8.8 \pm 1.0$, $c_{44}^N = 2.5 \pm 0.4$, $c_{66}^N = 2.9 \pm 0.4$ [10^4 g/cm s^2] tabulated in Table I. Figure 3 shows the quality of fit, where the vertical axis is the measured value of $C_P(\theta, \phi)$ and the horizontal axis is $C_P(\theta, \phi)$ calculated using the above c_{ij}^N for each crystal orientation (θ, ϕ). It should be noted that the elastic stiffness for pure longitudinal strain, c_{11}^N and c_{33}^N, were larger than those for shear strain, c_{44}^N and c_{66}^N.

TABLE I. The temperature-independent lattice parts of elastic stiffness c_{ij}^L, the coefficients of the temperature-dependent part c_{ij}^N, $\Gamma_{ij}^{\langle c \rangle}$ defined by Eq. (8).

ij	11	33	12	13	44	66	
c_{ij}^L	2.21		1.84		1.08		[$\times 10^8$ g/cm s^2]
c_{ij}^N	3.4 ± 1.0	7.4 ± 1.0	4.7 ± 1.7	8.8 ± 1.0	2.5 ± 0.4	2.9 ± 0.4	[$\times 10^4$ g/cm s^2]
$\Gamma_{ij}^{\langle c \rangle}$	103	224	142	267	76	88	

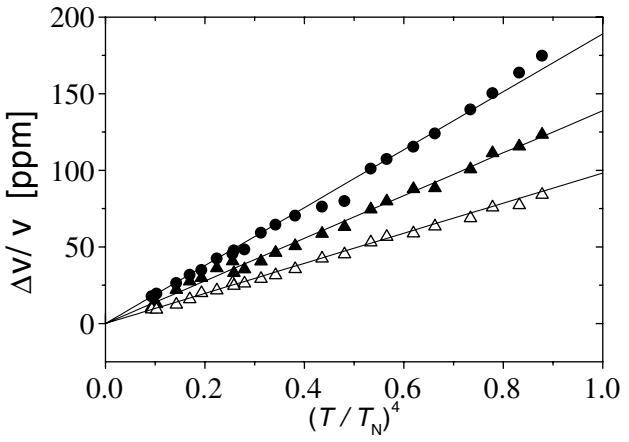

FIG. 1. Relative sound velocity change $\frac{\Delta v}{v}$ as a function of $(T/T_N)^4$ for three sound modes: longitudinal (filled circle), fast transverse (filled triangle), and slow transverse (open triangle) modes. The crystal orientation against $\hat{k}$ is $\theta = 20.0°$, $\phi = 11.2°$.

Next, we relate the measured coefficient of c_{ij}^N with Grüneisen constants for exchange constants. We write the internal energy of solid ^{3}He as follows:

$$U = U_0 + U_1(T), \tag{5}$$

where U_0 is the temperature-independent part of the internal energy and $U_1(T)$ is the temperature-dependent nuclear-spin part, which is given below T_N by

$$U_1(T) = \frac{\pi^2 k_B^4}{15\hbar^3\langle c\rangle^3} T^4, \tag{6}$$

where $\langle c\rangle$ is the spin wave velocity averaged over all angles, that is, $\langle c\rangle = \langle c_\perp^2 c_\parallel\rangle^{1/3}$, where $c_\perp$ and $c_\parallel$ stand for spin wave velocity perpendicular and parallel to the $\hat{l}$. From the melting pressure measurement, $\langle c\rangle = 7.8$ cm/ sec [12] is obtained after their data is scaled to $T_N = 0.93$ mK of the Greywall's temperature scale [7]. The adiabatic elastic stiffness is written by

$$c_{ij} = \frac{\partial^2 U_0}{\partial\epsilon_i\partial\epsilon_j}\bigg|_s + \frac{\partial^2 U_1}{\partial\epsilon_i\partial\epsilon_j}\bigg|_s = c_{ij}^L + c_{ij}^N\left(\frac{T}{T_N}\right)^4. \tag{7}$$

where the suffix S stands for the derivative under an adiabatic condition. The $U_1(T)$ depends on molar volume only through $\langle c\rangle$, and the derivative of $U_1(T)$ by strain ϵ_i appears through those of $\langle c\rangle$. The second derivative of $\langle c\rangle$ with respect to ϵ_i is defined as follows:

$$\Gamma_{ij}^{\langle c\rangle} \equiv \frac{1}{\langle c\rangle}\frac{\partial^2\langle c\rangle}{\partial\epsilon_i\partial\epsilon_j}. \tag{8}$$

When Eqs. (6)–(8) are combined, $\Gamma_{ij}^{\langle c\rangle}$ is related with $c_{ij}^N(\frac{T}{T_N})^4$ as

$$c_{ij}^N\left(\frac{T}{T_N}\right)^4 = \Gamma_{ij}^{\langle c\rangle} U_1(T). \tag{9}$$

We obtained $\Gamma_{11}^{\langle c\rangle} = 103$, $\Gamma_{33}^{\langle c\rangle} = 224$, $\Gamma_{12}^{\langle c\rangle} = 142$, $\Gamma_{13}^{\langle c\rangle} = 267$, $\Gamma_{44}^{\langle c\rangle} = 76$, and $\Gamma_{66}^{\langle c\rangle} = 88$, as tabulated in Table I.

There are four-independent Grüneisen constants of $\langle c\rangle$, $\gamma_i^{\langle c\rangle} \equiv \frac{1}{\langle c\rangle}[(\partial\langle c\rangle)/(\partial\epsilon_i)]$, which are γ_1, γ_3, γ_4, and γ_6, and $\gamma_2 = \gamma_1$, $\gamma_5 = \gamma_4$ under the tetragonal symmetry. Assuming $[(\partial\gamma_i^{\langle c\rangle})/(\partial\epsilon_j)] = 0$, we obtain the relations, $\Gamma_{11}^{\langle c\rangle} = \Gamma_{12}^{\langle c\rangle}$, and $\Gamma_{13}^{\langle c\rangle} = \sqrt{\Gamma_{11}^{\langle c\rangle}\Gamma_{33}^{\langle c\rangle}}$. We extract the $\gamma_1^{\langle c\rangle} = 12$, $\gamma_3^{\langle c\rangle} = 16$ from $\Gamma_{11}^{\langle c\rangle}$, $\Gamma_{33}^{\langle c\rangle}$, $\Gamma_{12}^{\langle c\rangle}$, and $\Gamma_{13}^{\langle c\rangle}$, and

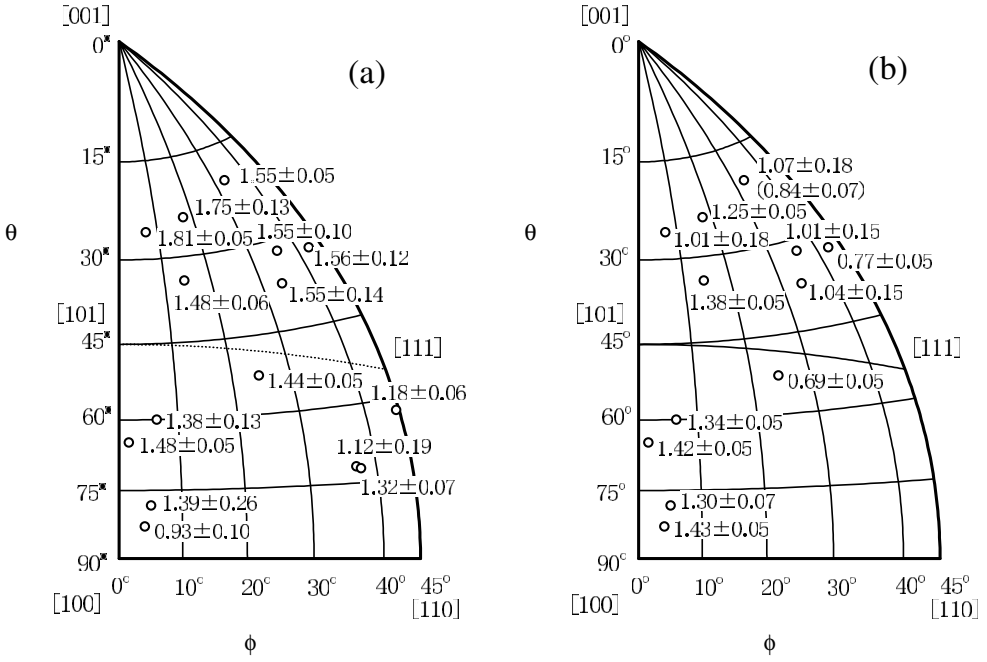

FIG. 2. The coefficient $C_p(\theta, \phi)$ of (a) longitudinal and (b) transverse sound velocity change in [$\times 10^{-4}$] on stereographic projection of 1/16 of the reference sphere. The value in parenthesis in graph (b) is for the slow mode and others are all for the fast mode.

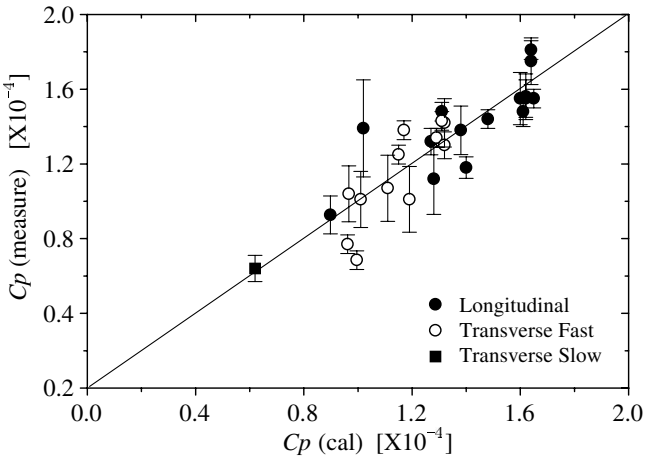

FIG. 3. The measured coefficients of the temperature-dependent sound velocity, C_P (measure), are plotted against the calculated coefficient, C_P (cal), using c_{ij}^N tabulated in Table I with tetragonal symmetry. The parameter is listed in Table I.

$\gamma_4^{\langle c\rangle} = 9$, $\gamma_6^{\langle c\rangle} = 9$ from $\Gamma_{44}^{\langle c\rangle}$, $\Gamma_{66}^{\langle c\rangle}$. The Grüneisen constant for pure compression (dilation) along $\hat{l}$, $\gamma_3^{\langle c\rangle} = 16$, is close to the usual Grüneisen constant ($\simeq 18$) for J and is larger than $\gamma_1^{\langle c\rangle} = 12$ for that perpendicular to $\hat{l}$. The Grüneisen constants for shear strains, $\gamma_4^{\langle c\rangle} = \gamma_6^{\langle c\rangle} = 9$ are almost half of 18 and are smaller than $\gamma_1^{\langle c\rangle}$ and $\gamma_3^{\langle c\rangle}$. The observed $\Gamma_{13} = 267$ are significantly larger than $\sqrt{\Gamma_{11}^{\langle c\rangle}\Gamma_{33}^{\langle c\rangle}} = 152$ and $(\partial\gamma_i^{\langle c\rangle})/(\partial\epsilon_j)$ may not be negligible.

Here, we analyze data by using the three-parameter model J_{NN}, J_T, and K_p. We neglect $(\partial\gamma_i^{\langle c\rangle})/(\partial\epsilon_j)$ for the simplicity of discussion and obtain relations of $\gamma_i^{\langle c\rangle}$ with the Grüneisen constants of the multiple-spin-exchange constants γ_i^J. Analytic expression for the spin wave velocities, $c_\parallel$ and $c_\perp$, are given by Ref. [13]. We assume the lattice is bcc; i.e., there is no Jahn-Teller deformation due to the onset of U2D2 and thus the spin-exchange Hamiltonian is isotropic. We introduce differences in the derivatives of the exchange constants by strain ϵ_i which depend on the relative orientation between the direction of the next-nearest neighbor (n.n.n) and ϵ_i. For instance, we distinguish $\gamma_3^{J_T^{(z)}} = (d\ln J_T^{(z)})/(d\ln\epsilon_3)$, where the n.n.n is parallel to ϵ_3, from $\gamma_1^{J_T^{(z)}} = (d\ln J_T^{(z)})/(d\ln\epsilon_1)$, where it is perpendicular to ϵ_1. Similarly, $\gamma_4^{J_T^{(z)}} = (d\ln J_T^{(z)})/(d\ln\epsilon_4)$ is different from $\gamma_6^{J_T^{(z)}} = (d\ln J_T^{(z)})/(d\ln\epsilon_6)$. The expressions for $\gamma_i^{\langle c\rangle}$ can be described by using the multiple-spin-exchange model but is rather complicate. Here we focus on the difference between $\gamma_1^{\langle c\rangle}$ and $\gamma_3^{\langle c\rangle}$, or $\gamma_4^{\langle c\rangle}$ and $\gamma_6^{\langle c\rangle}$.

$$\gamma_i^{\langle c\rangle} - \gamma_j^{\langle c\rangle} = -\frac{2J_T}{3}\left(\frac{3}{f} + \frac{1}{g_1} + \frac{2}{g_2}\right)(\gamma_i^{J_T^{(z)}} - \gamma_j^{J_T^{(z)}}) - \frac{2K_p}{3g_2}(\gamma_i^{K_p^{(z)}} - \gamma_j^{K_p^{(z)}}), \quad (10)$$

where, hereafter, $\{i, j\} = \{1, 3\}$ or $\{4, 6\}$ and

$$f = 2(J_{NN} - 10J_T + 6K_p),$$
$$g_1 = -\{(J_{NN} - 6J_T)(J_{NN} - 6J_T + 6K_p)\}/K_p - 4J_T,$$
$$g_2 = 8J_T - 2K_p. \quad (11)$$

In the three-parameter-exchange model, the difference in $\gamma_i^{\langle c\rangle} - \gamma_j^{\langle c\rangle}$ is related only with $\gamma_i^{J_T^{(z)}} - \gamma_j^{J_T^{(z)}}$ and $\gamma_i^{K_p^{(z)}} - \gamma_j^{K_p^{(z)}}$ since the Hamiltonian is isotropic. In the case that $[(2J_T)/3][(3/f) + (1/g_1) + (2/g_2)] \simeq 5 \gg (2K_p)/(3g_2) \simeq 0.2 > 0$ (this is the case for Ceperly and Jucci's parameters), the difference in $\gamma_i^{\langle c\rangle} - \gamma_j^{\langle c\rangle}$ comes mainly from the first term in Eq. (10). Our results, $\gamma_3^{\langle c\rangle} > \gamma_1^{\langle c\rangle}$ and $\gamma_4^{\langle c\rangle} \sim \gamma_6^{\langle c\rangle}$, indicate that $\gamma_1^{J_T^{(z)}} > \gamma_3^{J_T^{(z)}}$ and $\gamma_4^{J_T^{(z)}} \sim \gamma_6^{J_T^{(z)}}$. The difference $|\gamma_i^{J_T^{(z)}} - \gamma_j^{J_T^{(z)}}|$ is enhanced by a factor of 5 to $|\gamma_i^{\langle c\rangle} - \gamma_j^{\langle c\rangle}|$ and is a very small value. However, the factor is very sensitive to the choice of the exchange constants. It should be noted that the enhancement factor disappears in Eq. (10) if there is a common Grüneisen constant to each acoustic deformation for all exchange constants. It is neccessary to theoretically calculate Grüneisen constants to compare our data.

We would like to thank Professor Ohmi and Dr. Furukawa for useful discussions. This work is partly supported by the Grants-in-Aid for Scientific Research from the Ministry of Education, Culture, Sports, Science and Technology, Japan.

[1] D. M. Ceperley and G. Jacucci, Phys. Rev. Lett. **58**, 1648 (1987); **59**, 380 (1987).
[2] M. Roger, J. H. Hetherington, and J. M. Delrieu, Rev. Mod. Phys. **55**, 1 (1983); M. Roger, Phys. Rev. B **30**, 6432 (1984).
[3] N. Gov and E. Polturak, J. Low Temp. Phys. **128**, 55 (2002).
[4] For recent data, see E. R. Dobbs, *Helium Three* (Oxford University Press, Oxford, 2000), pp. 848–849.
[5] R. Nomura *et al.*, Phys. Rev. Lett. **85**, 2977 (2000).
[6] A. Fartash and J. M. Goodkind, Phys. Rev. Lett. **56**, 1389 (1986).
[7] D. v. S. Greywall, Phys. Rev. B **33**, 7520 (1986).
[8] D. D. Osheroff, M. C. Cross, and D. S. Fisher, Phys. Rev. Lett. **44**, 792 (1980).
[9] R. Wanner, Phys. Rev. A **3**, 448 (1971).
[10] M. C. Cross and D. S. Fisher, Rev. Mod. Phys. **57**, 881 (1985).
[11] W. Ni *et al.*, J. Low Temp. Phys. **100**, 167 (1995).
[12] D. D. Osheroff and C. Yu, Phys. Lett. **77A**, 458 (1980).
[13] K. Iwahashi and Y. Masuda, J. Phys. Soc. Jpn. **50**, 2508 (1981).